Materials for Agricultural Gas Sensors

Contributor: Calvin Love, Haleh Nazemi, Eman El-Masri, Arezoo Emadi

A sensing material employed as a gas sensor will react with multiple gases, and for this reason, multiple sensing materials are employed in a network of gas sensors known as an electronic nose (eNose) system. By recording the response of this network of gas sensors, a signature which relates to the target analyte is detected, mitigating the issue of selectivity.

1. Introduction

A significant proportion of agricultural fruits and vegetables originates from greenhouses, with increasing frequency and a steady rise in harvest land area for crops produced via greenhouse methods [1]. One main reason for the significance of greenhouse practices is that they offer the advantage of year-round production, enabling financial stability for the grower [2]. During the phases of plant growth and storage in agricultural greenhouse environments, there are various volatiles that can affect growth quality and prolong the shelf life of crops, including ethylene, carbon dioxide (CO_2) hydrogen sulfide (H_2S), ethanol and water vapor (humidity) [3][4][5].

Because of the key roles played by these small molecules, it is important to monitor them in plant growth environments such as greenhouses, as well as in storage and transport environments. Monitoring of such volatiles can be achieved with sensors that typically require the use of a sensing material. According to B. Eggins, there are three general classifications of sensors containing sensing materials: (1) chemical sensors where the analyte interacts with the sensing material via chemical or physical responses, (2) physical sensors which measure a physical change such as length, weight and temperature and (3) biosensors, which utilize a biosensing element to measure chemical substances [6]. The chemical sensing technologies (including electrochemical sensors) often work by transforming gas concentrations into an electrical signal such as current (amperometric sensors), potential (voltammetric), resistance (chemoresistive sensors) and frequency response (capacitive sensors, acoustic sensors and thermal magnetic) [7][8][9].

Some commonly reported classes of sensing materials are metal oxides [10][11], polymers (conducting and non-conducting) [12][13], and carbon nanotubes (including other allotropes of carbon such as graphene) [14][15]. There are also reports of multiple classes used simultaneously, like metal oxide/CNTs composites [16], polymer/graphene composites [17] and less commonly used materials like metal-organic frameworks (MOFs) [18] and ionic liquids [19]. This review discusses the above-mentioned types of sensing materials in terms of their method of application onto a sensor, physical properties once applied and mechanism of operation for detecting relevant agricultural analytes such as ethylene, CO_2, ethanol, H_2S and water vapor. It is observed that some of these sensing materials demonstrate sensitivity and selectivity to certain target analytes, while others are responsive to multiple analytes present in an agricultural greenhouse environment.

2. Sensing Materials for Target Analyte Detection

2.1. Ethylene Detection

Many metal oxide materials have been developed and tested for the detection of ethylene. Li, Jin et al. reported the use of porous zinc oxide nanosheets (ZnO NS) as an ethylene sensing material to determine fruit ripeness [20]. Another notable metal oxide; commercially available tin oxide, SnO_2 nanoparticles, reported by Agarwal and colleagues, show the capability of detecting ethylene at 20 ppm levels with CO_2, SO_2, NH_3, NO_2, and H_2S, NH as an interfering gas at concentrations ranging from 1000–3000 ppm at room temperature [11]. In regards to carbon allotropes, Swager et al. used single-walled carbon nanotubes (SWCNTs) functionalized with 4-pyridyl moieties as a sensing material in monitoring the senescence in red carnation via the detection of trace levels of ethylene gas [21]. In a different class of viable materials, the use of commercially available ionic liquids (ILs), such as 1-butyl-3-methylimidazolium bis(trifluoromethyl sulfonyl)imide ([BMIM][NTf$_2$]), is reported by Zevenbergen et al.

2.2. Carbon Dioxide Detection

A wide variety of metal oxide sensing materials have been reported for their use in CO_2 detection. One such sensing material under this class is reported by Karthik et al., who developed a Zinc oxide (ZnO) sensing material, synthesized by the thermal decomposition of precursors such as zinc acetate and zinc nitrate [22]. Another notable metal oxide for use in

CO_2 detection is cerium oxide (CeO_2) nanospheres [23]. Karthik et al. coated a g-C_3N_4 nanosheet with TiO_2, forming a hybrid 2D sensing material for the purposes of CO_2 detection [24].

Baltrusaitis et al. reported a material under the polymer class; methylated poly(ethylene) imine (mPEI) for CO_2 detection, synthesized by previously reported work [13]. This polymer is also sensitive to sulfur dioxide (SO_2) detection, to which the material shows a lower sensory response. Among the viable ionic liquid sensing materials is 1-ethyl-3-methylimidazolium bis (trifluoromethyl-sulfonyl)-imide (EMIM[NTf_2]), which was investigated by Bhide et al. [25]. Wei et al. reported a rather exotic sensing material, which was a functionalized pillar[5]arene/bipyridine salt for the detection of CO_2 at a detection limit of 2.2 ppm [26].

2.3. Hydrogen Sulfide Detection

Under the metal oxide material class, Li et al. used indium oxide (In_2O_3) nano-cubes for sensing H_2S at room 25 °C and 100 °C [27]. Synthesis of this material involved a cetyltrimethyl ammonium bromide (CTAB)-assisted solvothermal and subsequent calcination process. This material has a very impressive 5 ppb limit of detection and interestingly, selectivity between NO_2 (also able to detect) and H S sensing can be tuned using temperature (25 °C versus 100 °C). A viable material under the polymer material class—polyaniline/metal chloride nanofiber composites as sensing materials for H_2S detection—was reported by Virji et al. [28]. Among the carbon allotrope material class, Asad et al. reported single-walled carbon nanotubes (SWCNTs) modified with copper nanoparticles for H_2S detection [29].

2.4. Ethanol Detection

Among the metal oxide class, palladium/titanium oxide (Pd/TiO_2) nanorod arrays and tin sulfide (SnS) nanoflakes were reported by Dutta [30] and Afsar [31]. The Pd/TiO_2 nanorod arrays are also sensitive to 2-propanol and able to detect down to 1 ppm of theses alcohol vapors. Within the polymer material class, Yoon et al. used poly(styrene-co-allyl alcohol) (PSAA) as a sensing material (other materials also shown) in a wireless sensor to detect ethanol, which proved to be cross sensitive to acetone and ethylene [32]. Among ionic liquids, Xu et al. reported a viable material for the detection of ethanol are alkyl-imidazolium halide [33], which can be synthesized using simple solution synthetic methods, or can be procured commercially.

2.5. Humidity Detection

Within the metal oxide material glass, Zhang et al. reported a graphene oxide/polymer composite for humidity detection [10]. Shifting focus to the polymer sensing materials, Zhao et al. reported MWCNTs functionalized with poly-L-lysin (PLL) to be a viable sensing material for humidity detection [34]. Qi et al. demonstrated a material under the carbon allotrope material class known as chitosan-wrapped multi-walled carbon nanotubes (MWCNTs-CS) for detecting humidity [15]. Duan et al. reported Halloysite nanotubes as a sensing material for humidity which has a dynamic range of 0–91.5% RH [35]. For use in fibre-optic sensing applications, a wide range of sensing materials is available for humidity detection. This group of gas sensors employs several techniques, including fibre grating, evanescent wave monitoring, interferometric approach and absorption measurements, as well as hybrid sensors [36][37][38][39].

3. Deposition Methods

One of the challenges in sensor development for agricultural monitoring is to apply the developed sensing material to the active area of a sensor; this is often referred to as material deposition. In addition, since there are different mechanisms of operation for gas sensors due to their different structures, including capacitive and piezoelectric-based, QCM, chemiresistive and fibre-optic gas sensors, particular deposition techniques should be utilized to improve sensors' performance in static and dynamic operations. Therefore, the sensor's mechanism of operation, along with desired sensing material thickness and active area, which agree to the optimum sensor's response point, can define the potential deposition technique. The most common deposition method observed using all the sensing materials mentioned in previous sections, is drop-coating. This technique is mostly used in chemiresistive gas sensors; obtaining a layer of few nanometers sensing material is not required [23][24]. Other common methods that are also suitable and utilized to deposit the aforementioned sensing materials include spin-coating, dip-coating, spraying, electro-spinning, and inkjet printing, as shown in Table 1. Gas sensors such as capacitive-based structures, which have a thick layer of sensing material, can have a negative impact on their operation benefit from the inkjet printing technique [40].
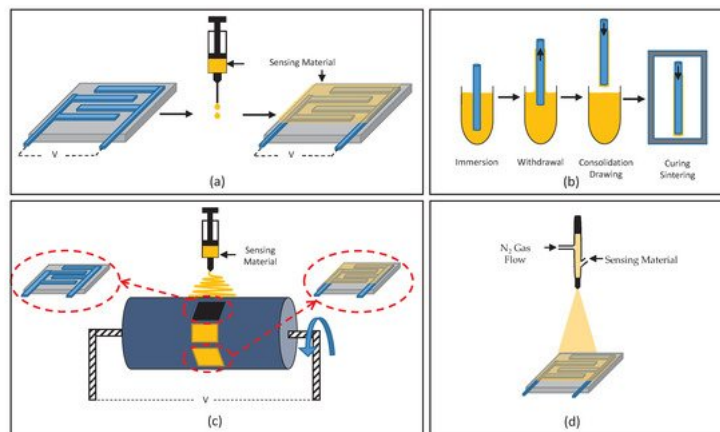
Figure 1. Schematic illustration of deposition methods: (**a**) drop-coating, (**b**) dip-coating, (**c**) electro-spinning and (**d**) spraying.

Table 1. Material deposition methods, sensing technologies, sensor performance parameters and operating temperatures with various sensing materials and target analytes in gas phase.

Sensing Material	Target Analyte	Sensing Technology	Deposition Method	Material Thickness	Dynamic Range & Limit of Detection	Recovery Time	Operating Temperature	Long-Term Stability	Sensitivi (Output/Inp
BMIM-NTf$_2$	Ethylene	Amperometric	Drop-coating	63 μm	760 ppb–10 ppm	-	22 °C	-	51 pA/pp
Porous ZnO NS	Ethylene	Chemiresistive	Dip-coating	10 nm	5–2000 ppm	20 s	350–500 °C	30 days	0.6 μA/pp
LaFeO$_3$	Ethylene	Chemiresistive	Screen printing	37–38.3 μm	25–5000 ppm	~1 s	20–200 °C	-	0.4Ω/ppr
SWCNTs	Ethylene	Chemiresistive	-	1 μL	0.5–50 ppm	-	4 °C	16 days	1.2%R/pp
SnO$_2$ nanoparticles	Ethylene	Chemicapacitive	Dip-coating/Sputtering	1300 nm	20–100 ppm	~10 s	22 °C	-	0.0531 pF/
PtTiO$_2$	Ethylene	Magnetoelastic	Dip-Coating	31–155 nm	0.5–50 ppm	-	19 °C	-	8.5 Hz/pp
ZnO	CO$_2$	Chemiresistive	Spray pyrolysis	8.3 nm	50–1000 ppm	100 s	300 °C	-	800 Ω/ppr
PEDOT PSS/graphene	CO$_2$	Chemiresistive	Calibrated spreader	10 μm	4.7–4500 ppm	-	35–65 °C	-	0.004–0.0047%R/%
TIO$_2$ coated g-C$_3$N$_4$ NS	CO$_2$	Chemiresistive	Drop-coating	30 nm	100–2500 ppm	35 s	22 °C	60 days	406 μΩ/pp
CeO$_2$	CO$_2$	Chemiresistive	Drop-coating	170–210 nm diam.	150–2400 ppm	~1 s	100–250 °C	-	4.88 kΩ/p
EMIM[NTF$_2$]	CO$_2$	Chemicapacitive	Dip-coating	<1 μm	50,000–1,000,000 ppm	38.5 s	Room temperature	-	29 pF/pp
HPTS	CO$_2$	Fibre-Optic	Dip-coating	>1 μm	300–300,000 ppm	50–100 s	22 °C	-	0.00055 a.u./ppr
mPEI	CO$_2$	Resonator	Spin coating	-	0.011%	-	-	-	8 Hz/ppr
CuO,Fe$_2$O$_3$	H$_2$S	Amperometric	-	-	10ppm	-	−15 °C–65 °C	-	700 μA/pp
CNTs/SnO$_2$/CuO	H$_2$S	Chemiresistive	Spin-coating	>6 nm	10–80 ppm	10 min	25 °C	-	4.41Ω/pp
SnO$_2$ nanofibres	H$_2$S	Chemiresistive	Electro-spinning	150 nm diam.	0.1–1 ppm	230 s	200–350 °C	-	970kΩ/pp
Zn$_2$SnO$_4$ NS	H$_2$S	Chemiresistive	Dip-coating	100 nm	5–1000 ppb	1300 s	133–170 °C	60 days	1.08MΩ/p
In$_2$O$_3$	H$_2$S	Chemiresistive	Dip-coating	100 um	5 ppb	5 min	25–100 °C	30 days	13.02 kΩ/p

Sensing Material	Target Analyte	Sensing Technology	Deposition Method	Material Thickness	Dynamic Range & Limit of Detection	Recovery Time	Operating Temperature	Long-Term Stability	Sensitivi (Output/In
WO_3, PPy	H_2S	Chemiresistive	-	50–100 nm	200 ppm	>1 day	90 °C	-	490 µV/pp
SWCNTs	H_2S	Chemiresistive	Spin-coating	1–2 nm diam.	5 ppm–150 ppm	10–15 s	20 °C	-	0.47%R/p
ZnO Nanowires	Ethanol	Chemiresistive	Spin-coating	25 nm diam.	1–200 ppm	120 s	300 °C	-	644Ω/pp
SnS	Ethanol	Chemiresistive	-	-	10 ppm	9 s	200 °C	6 weeks	0.27–13.5%R/p
Pd/TiO_2	Ethanol	Chemicapacitive	Nanorod growth	710–750 nm	1–100 ppm	2.4–3.8 s	100 °C	-	7.5%C/pp
SiO2/Si NW	Ethanol	MGFET	vapor-liquid-sold growth	16 nm diam.	26–2000 ppm	4 min	60 °C	-	16–40 pA/
PSAA	Ethanol	Resonator	Drop-coating	19.9 nm	13.3 ppm	20 min	24 °C	-	1.5 Hz/pp
CuO particles	Water Vapor	Chemiresistive	Drop-coating	140 µm	33–90%RH	-	22 °C	-	0.5–30kΩ/%
WS_2 NS	Water Vapor	Chemiresistive	Drop-coating	6 nm	8–85%RH	30–140 s	-	several weeks	580 MΩ/%
MWCNTs-CS	Water Vapor	Chemiresistive	-	-	11–95%RH	-	Room temperature	-	2.4 mΩ/%
MWCNTs-PLL	Water Vapor	Chemiresistive	Drop-coating	-	0–91.5%RH	-	Room temperature	-	3.78kΩ/%
MoS_2/ND	Water Vapor	Chemicapacitive	-	-	11–97%RH	-	Room temperature	-	6.5 nF/%
SPEEK	Water Vapor	Impedance-based	Drop-coating	20 µm	11–95%RH	130 s	22 °C	30 days	12-120MΩ/%
TiO_2 Nanowires	Water Vapor	Impedance-based	Dip-coating	40–50 nm	12–97%RH	<2 min	17–35 °C	250 days	144kΩ/%
Silica/di-ureasil FBG	Water Vapor	Fibre-Optic	Dip-coating	450–591 µm	5–95%RH	-	5–40 °C	1 year	1.25–7.1 pm/%RI
PI	Water Vapor	Fibre-Optic	Dip-coating	450–591 µm	5-95%RH	-	−15–20 °C	-	1.85–2.2 pm/%RI
$Al_2O_3^+/PSS^-$ nano-film	Water Vapor	Fibre-Optic	ESA	84nm	22–39%RH	-	24.5 °C	-	1.43 nm/%
SiO_2	Water Vapor	Fibre-Optic	ESA	300 nm	20–80%RH	150ms	10–40 °C	-	67.33–451 pm/%RI
$CaCl_2$	Water Vapor	Fibre-Optic	-	3 µm	55–95%RH	-	30 °C	-	1.36 nm/%
$CoCl_2$	Water Vapor	Fibre-Optic	Drop-coating	10 µm	50–95%RH	~40 s	25 °C	-	67–200 pm/%RI
HEC/PVDF	Water Vapor	Fibre-Optic	Dip-impregnation	-	40–90%RH	-	28 °C	-	0.196 dB/%
PAA Nanowires	Water Vapor	Fibre-Optic	Electrospinning	-	30–95%RH	210 ms	25 °C	-	0.01 dB/%
ZnO Nanorods	Water Vapor	Fibre-Optic	Dip-coating	2.5 µm	10–95%RH	-	25 °C	-	0.0007–0.0057%P/%
PVA	Water Vapor	Fibre-Optic	Dip-coating	8 µm	20–95%RH	500 ms	20–100 °C	7 days	25–980 pm/%RH
PEO	Water Vapor	Fibre-Optic	Dip-coating	-	85–90%RH	~1 s	22 °C	-	1.17 dB/%
Silica/methylene blue	Water Vapor	Fibre-Optic	Dip-coating	-	1.1-4.1%RH	<30 s	18 °C	-	0.0087 a.u./%RI

Sensing Material	Target Analyte	Sensing Technology	Deposition Method	Material Thickness	Dynamic Range & Limit of Detection	Recovery Time	Operating Temperature	Long-Term Stability	Sensitivi (Output/In
Ag-Polyaniline	Water Vapor	Fibre-Optic	Dip-coating	15–30 nm diam.	5-95%RH	90s	25–30 °C	-	10–29 mV/%
PGA/poly-lysine	Water Vapor	Fibre-Optic	Soaked in polymer	1 µm	50–92.9%RH	5.8 s	-	-	0.01 dBm/%
ZnO	Water Vapor	Fibre-Optic	Dip/Spin-coating	70–80 nm diam.	5–50%RH	35 s	22 °C	-	0.45%dB/%
Co/Polyaniline	Water Vapor	Fibre-Optic	Dip-coating	10.4 µm	20–92%RH	1 min	30 °C	-	0.024–3.4 mV/%RI
Gelatin	Water Vapor	Fibre-Optic	Dip-coating	80 nm	9–94%RH	~50 s	22 °C	-	0.167 dBm/%R
Chitosan	Water Vapor	Fibre-Optic	Dip-coating	-	20–80%RH	-	25 °C	-	81 pm/%F

4. Conclusions

As new sensing materials and technologies continue to be developed for use in greenhouse environments, it will be essential to demonstrate their operation in representative environments that explore long-term stability and cross-sensitivity under realistic conditions. The rapid advances in sensing materials, morphology, and structure, as well as transduction mechanisms are expected to address current limitations in performance and are expected to enable miniaturized, low-power sensors capable of achieving wireless, distributed sensor networks for the continuous monitoring of agriculture environments. Further experimentation on the listed sensing materials should be implemented, recording the sensitivity of each material to their respective analyte over a long period of time to validate the usefulness of each material for greenhouse applications. Furthermore, the material's solubility in water and sensitivity to elevated RH can help determine where the sensor ought to be located within the greenhouse.

References

1. Wang, Z. Statistical Overview of the Canadian Greenhouse Vegetable Industry 2015 Prepared by: Market Analysis and Information Section Horticulture and Cross Sectoral Division Agriculture and Agri-Food Canada; Technical Report; Agriculture and Agri-Food Canada: Guelph, ON, Canada, 2016.

2. Jansen, R.; Takayama, K.; Wildt, J.; Hofstee, J.W.; Bouwmeester, H.; van Henten, E. Monitoring Crop Health Status at Greenhouse Scale on the Basis of Volatiles Emitted from the Plants. Environ. Control Biol. 2009, 47, 87–100.

3. Burg, S.P.; Burg, E.A. Role of Ethylene in Fruit Ripening. Plant Physiol. 1962, 37, 179–189.

4. Roy, J.K.; Akram, R.; Shuvo, M.A.F.; Khatun, H.; Awal, M.S.; Sarker, M. Effect of Ethanol Vapor on Ripening of Tomato. Agric. Eng. Int. CIGR J. 2017, 19, 168–175.

5. Kawamitsu, Y.; Yoda, S.; Agata, W. Humidity Pretreatment Affects the Responses of Stomata and CO2 Assimilation to Vapor Pressure Difference in C3 and C4 Plants. Plant Cell Physiol. 1993, 34, 113–119.

6. Eggins, B.R. Chemical Sensors and Biosensors; John Wiley & Sons: Chichester, UK, 2002; Volume 2.

7. Balasingam, J.A.; Swaminathan, S.; Nazemi, H.; Love, C.; Birjis, Y.; Emadi, A. Chemical Sensors: Gas Sensors, Acoustic Sensors. In Reference Module in Biomedical Sciences; Elsevier: Amsterdam, The Netherlands, 2021.

8. Rayl, M.; Wojtowicz, P.J.; Hanson, H.D. Magnetic gas sensor. AIP Conf. Proc. 1976, 29, 628–629.

9. Janata, J. Principles of Chemical Sensors; Springer Science & Business Media: New York, NY, USA, 2010.

10. Wang, M.; Zhang, D.; Yang, A.; Wang, D.; Zong, X. Fabrication of polypyrrole/graphene oxide hybrid nanocomposite for ultrasensitive humidity sensing with unprecedented sensitivity. J. Mater. Sci. Mater. Electron. 2019, 30, 4967–4976.

11. Agarwal, M.; Balachandran, M.D.; Shrestha, S.; Varahramyan, K. SnO2 nanoparticle-based passive capacitive sensor for ethylene detection. J. Nanomater. 2012, 2012, 145406.

12. Ding, B.; Yamazaki, M.; Shiratori, S. Electrospun fibrous polyacrylic acid membrane-based gas sensors. Sens. Actuators Chem. 2005, 106, 477–483.

13. Barauskas, D.; Pelenis, D.; Vanagas, G.; Viržonis, D.; Baltrušaitis, J. Methylated poly(Ethylene)imine modified capacitive micromachined ultrasonic transducer for measurements of CO2 and SO2 in their mixtures. Sensors 2019, 19, 3236.

14. Gargiulo, V.; Alfano, B.; Di Capua, R.; Alfé, M.; Vorokhta, M.; Polichetti, T.; Massera, E.; Miglietta, M.L.; Schiattarella, C.; Di Francia, G. Graphene-like layers as promising chemiresistive sensing material for detection of alcohols at low

concentration. J. Appl. Phys. 2018, 123, 024503.

15. Qi, P.; Xu, Z.; Zhang, T.; Fei, T.; Wang, R. Chitosan wrapped multiwalled carbon nanotubes as quartz crystal microbalance sensing material for humidity detection. J. Colloid Interface Sci. 2020, 560, 284–292.

16. Zhao, Y.; Zhang, J.; Wang, Y.; Chen, Z. A Highly Sensitive and Room Temperature CNTs/SnO2/CuO Sensor for H2S Gas Sensing Applications. Nanoscale Res. Lett. 2020, 15, 1–8.

17. Wu, Z.; Zhu, S.; Dong, X.; Yao, Y.; Guo, Y.; Gu, S.; Zhou, Z. A facile method to graphene oxide/polyaniline nanocomposite with sandwich-like structure for enhanced electrical properties of humidity detection. Anal. Chim. Acta 2019, 1080, 178–188.

18. Tang, Y.; Chen, J.; Wu, H.; Yu, J.; Jia, J.; Xu, W.; Fu, Y.; He, Q.; Cao, H.; Cheng, J. A highly fluorescent post-modified metal organic framework probe for selective, reversible and rapid carbon dioxide detection. Dyes Pigment. 2020, 172, 107798.

19. Zevenbergen, M.A.; Wouters, D.; Dam, V.A.T.; Brongersma, S.H.; Crego-Calama, M. Electrochemical sensing of ethylene employing a thin ionic-liquid layer. Anal. Chem. 2011, 83, 6300–6307.

20. Wang, L.P.; Jin, Z.; Luo, T.; Ding, Y.; Liu, J.H.; Wang, X.F.; Li, M.Q. The detection of ethylene using porous ZnO nanosheets: Utility in the determination of fruit ripeness. New J. Chem. 2019, 43, 3619–3624.

21. Fong, D.; Luo, S.X.; Andre, R.S.; Swager, T.M. Trace Ethylene Sensing via Wacker Oxidation. Acs Cent. Sci. 2020.

22. Karthik, T.V.; Hernández, A.G.; Kudriavtsev, Y.; Gómez-Pozos, H.; Ramírez-Cruz, M.G.; Martínez-Ayala, L.; Escobosa-Echvarria, A. Sprayed ZnO thin films for gas sensing: Effect of substrate temperature, molarity and precursor solution. J. Mater. Sci. Mater. Electron. 2020, 1–11.

23. Zito, C.A.; Perfecto, T.M.; Dippel, A.C.; Volanti, D.P.; Koziej, D. Low-Temperature Carbon Dioxide Gas Sensor Based on Yolk-Shell Ceria Nanospheres. ACS Appl. Mater. Interfaces 2020, 12, 17745–17751.

24. Karthik, P.; Gowthaman, P.; Venkatachalam, M.; Saroja, M. Design and fabrication of g-C3N4 nanosheets decorated TiO2 hybrid sensor films for improved performance towards CO2 gas. Inorg. Chem. Commun. 2020, 119, 108060.

25. Bhide, A.; Jagannath, B.; Tanak, A.; Willis, R.; Prasad, S. CLIP: Carbon Dioxide testing suitable for Low power microelectronics and IOT interfaces using Room temperature Ionic Liquid Platform. Sci. Rep. 2020, 10, 1–12.

26. Zhu, W.B.; Wei, T.B.; Fan, Y.Q.; Qu, W.J.; Zhu, W.; Ma, X.Q.; Yao, H.; Zhang, Y.M.; Lin, Q. A pillar[5]arene-based and OH-dependent dual-channel supramolecular chemosensor for recyclable CO2 gas detection: High sensitive and selective off-on-off response. Dyes Pigment. 2020, 174, 108073.

27. Li, Z.; Yan, S.; Sun, M.; Li, H.; Wu, Z.; Wang, J.; Shen, W.; Fu, Y.Q. Significantly enhanced temperature-dependent selectivity for NO2 and H2S detection based on In2O3 nano-cubes prepared by CTAB assisted solvothermal process. J. Alloys Compd. 2020, 816, 152518.

28. Virji, S.; Fowler, J.D.; Baker, C.O.; Huang, J.; Kaner, R.B.; Weiller, B.H. Polyaniline Nanofiber Composites with Metal Salts: Chemical Sensors for Hydrogen Sulfide. Small 2005, 1, 624–627.

29. Asad, M.; Sheikhi, M.H.; Pourfath, M.; Moradi, M. High sensitive and selective flexible H2S gas sensors based on Cu nanoparticle decorated SWCNTs. Sens. Actuators B Chem. 2015, 210, 1–8.

30. Dutta, K.; Bhowmik, B.; Bhattacharyya, P. Resonant Frequency Tuning Technique for Selective Detection of Alcohols by TiO2 Nanorod-Based Capacitive Device. IEEE Trans. Nanotechnol. 2017, 16, 820–825.

31. Afsar, M.F.; Rafiq, M.A.; Tok, A.I. Two-dimensional SnS nanoflakes: Synthesis and application to acetone and alcohol sensors. RSC Adv. 2017, 7, 21556–21566.

32. Yoon, I.; Eom, G.; Lee, S.; Kim, B.K.; Kim, S.K.; Lee, H.J. A capacitive micromachined ultrasonic transducer-based resonant sensor array for portable volatile organic compound detection with wireless systems. Sensors 2019, 19, 1401.

33. Xu, X.; Li, C.; Pei, K.; Zhao, K.; Zhao, Z.K.; Li, H. Ionic liquids used as QCM coating materials for the detection of alcohols. Sens. Actuators B Chem. 2008, 134, 258–265.

34. Zhao, Q.; Yuan, Z.; Duan, Z.; Jiang, Y.; Li, X.; Li, Z.; Tai, H. An ingenious strategy for improving humidity sensing properties of multi-walled carbon nanotubes via poly-L-lysine modification. Sens. Actuators B Chem. 2019, 289, 182–185.

35. Duan, Z.; Zhao, Q.; Wang, S.; Huang, Q.; Yuan, Z.; Zhang, Y.; Jiang, Y.; Tai, H. Halloysite nanotubes: Natural, environmental-friendly and low-cost nanomaterials for high-performance humidity sensor. Sens. Actuators B Chem. 2020, 317, 128204.

36. Ascorbe, J.; Corres, J.; Arregui, F.; Matias, I. Recent Developments in Fiber Optics Humidity Sensors. Sensors 2017, 17, 893.

37. Alwis, L.; Sun, T.; Grattan, K.T.V. Optical fibre-based sensor technology for humidity and moisture measurement: Review of recent progress. Measurement 2013, 46, 4052–4074.

38. Yeo, T.L.; Sun, T.; Grattan, K.T.V. Fibre-optic sensor technologies for humidity and moisture measurement. Sens. Actuators A Phys. 2008, 144, 280–295.

39. Leal-Junior, A.; Frizera-Neto, A.; Marques, C.; Pontes, M. Measurement of Temperature and Relative Humidity with Polymer Optical Fiber Sensors Based on the Induced Stress-Optic Effect. Sensors 2018, 18, 916.

40. Liu, M.; Guo, S.; Xu, P.; Yu, H.; Xu, T.; Zhang, S.; Li, X. Revealing humidity-enhanced NH3 sensing effect by using resonant microcantilever. Sens. Actuators B Chem. 2018, 257, 488–495.

41. Alharbi, A.A.; Sackmann, A.; Weimar, U.; Bârsan, N. A highly selective sensor to acetylene and ethylene based on LaFeO3. Sens. Actuators B Chem. 2020, 303, 127204.

42. Alharbi, A.A.; Sackmann, A.; Weimar, U.; Bârsan, N. Acetylene- and Ethylene-Sensing Mechanism for LaFeO3 -Based Gas Sensors: Operando Insights. J. Phys. Chem. C 2020, 124, 7317–7326.

43. Zhang, R.; Tejedor, M.I.; Anderson, M.A.; Paulose, M.; Grimes, C.A. Ethylene Detection Using Nanoporous PtTiO2 Coatings Applied to Magnetoelastic Thick Films. Sensors 2002, 2, 331–338.

44. Andò, B.; Baglio, S.; Pasquale, G.D.; Pollicino, A.; Graziani, S.; Gugliuzzo, C.; Lombardo, C.; Marletta, V. Direct printing of a multi-layer sensor on PET substrate for CO2 detection. Energies 2019, 12, 557.

45. Chu, C.S.; Lo, Y.L. Fiber-optic carbon dioxide sensor based on fluorinated xerogels doped with HPTS. Sens. Actuators B Chem. 2008, 129, 120–125.

46. Zhang, P.; Zhu, H.; Xue, K.; Chen, L.; Shi, C.; Wang, D.; Li, J.; Wang, X.; Cui, G. H2S detection at low temperatures by Cu2O/Fe2O3 heterostructure ordered array sensors. RSC Adv. 2020, 10, 8332–8339.

47. Phuoc, P.H.; Hung, C.M.; Van Toan, N.; Van Duy, N.; Hoa, N.D.; Van Hieu, N. One-step fabrication of SnO2 porous nanofiber gas sensors for sub-ppm H2S detection. Sens. Actuators A Phys. 2020, 303, 111722.

48. Xu, T.T.; Zhang, X.F.; Dong, X.; Deng, Z.P.; Huo, L.H.; Gao, S. Enhanced H2S gas-sensing performance of Zn2SnO4 hierarchical quasi-microspheres constructed from nanosheets and octahedra. J. Hazard. Mater. 2019, 361, 49–55.

49. Geng, L. Gas sensitivity study of polypyrrole/WO3 hybrid materials to H2S. Synth. Met. 2010, 160, 1708–1711.

50. Wan, Q.; Li, Q.H.; Chen, Y.J.; Wang, T.H.; He, X.L.; Li, J.P.; Lin, C.L. Fabrication and ethanol sensing characteristics of ZnO nanowire gas sensors. Appl. Phys. Lett. 2004, 84, 3654–3656.

51. Shalev, G. The Electrostatically Formed Nanowire: A Novel Platform for Gas-Sensing Applications. Sensors 2017, 17, 471.

52. Paska, Y.; Stelzner, T.; Christiansen, S.; Haick, H. Enhanced Sensing of Nonpolar Volatile Organic Compounds by Silicon Nanowire Field Effect Transistors. ASC Nano 2021, 17, 45.

53. Park, S.; Yoon, I.; Lee, S.; Kim, H.; Seo, J.W.; Chung, Y.; Unger, A.; Kupnik, M.; Lee, H.J. CMUT-based resonant gas sensor array for VOC detection with low operating voltage. Sens. Actuators B Chem. 2018, 273, 1556–1563.

54. Malook, K.; Khan, H.; Ali, M.; Ihsan-Ul-Haque. Investigation of room temperature humidity sensing performance of mesoporous CuO particles. Mater. Sci. Semicond. Process. 2020, 113, 105021.

55. Leonardi, S.G.; Wlodarski, W.; Li, Y.; Donato, N.; Sofer, Z.; Pumera, M.; Neri, G. A highly sensitive room temperature humidity sensor based on 2D-WS2 nanosheets. FlatChem 2018, 9, 21–26.

56. Yu, X.; Chen, X.; Ding, X.; Yu, X.; Zhao, X.; Chen, X. Facile fabrication of flower-like MoS2/nanodiamond nanocomposite toward high-performance humidity detection. Sens. Actuators B Chem. 2020, 317, 128168.

57. Ru, C.; Gu, Y.; Li, Z.; Duan, Y.; Zhuang, Z.; Na, H.; Zhao, C. Effective enhancement on humidity sensing characteristics of sulfonated poly(ether ether ketone) via incorporating a novel bifunctional metal–organic–framework. J. Electroanal. Chem. 2019, 833, 418–426.

58. Wu, R.J.; Sun, Y.L.; Lin, C.C.; Chen, H.W.; Chavali, M. Composite of TiO2 nanowires and Nafion as humidity sensor material. Sens. Actuators B Chem. 2006, 115, 198–204.

59. Correia, S.F.H.; Antunes, P.; Pecoraro, E.; Lima, P.P.; Varum, H.; Carlos, L.D.; Ferreira, R.A.S.; André, P.S. Optical Fiber Relative Humidity Sensor Based on a FBG with a Di-Ureasil Coating. Sensors 2012, 12, 8847–8860.

60. Berruti, G.; Consales, M.; Cutolo, A.; Cusano, A.; Breglio, G.; Buontempo, S.; Petagna, P.; Giordano, M. Radiation hard humidity sensors for high energy physics applications using polymide-coated Fiber Bragg Gratings sensors. Sens. Actuators B Chem. 2011, 177, 94–102.

61. Zheng, S.; Zhu, Y.; Krishnaswamy, S. Fiber humidity sensors with high sensitivity and selectivity based on interior nanofilm-coated photonic crystal fiber long-period gratings. Sens. Actuators B Chem. 2013, 176, 264–274.

62. Viegas, D.; Hernaez, M.; Goicoechea, J.; Santos, J.; Araújo, F.; Arregui, F.; Matias, I. Simultaneous Measurement of Humidity and Temperature Based on an SiO2-Nanospheres Film Deposited on a Long-Period Grating In-Line With a Fiber Bragg Grating. IEEE Sens. J. 2010, 11, 162–166.

63. Fu, M.Y.; Lin, G.R.; Liu, W.F.; Wu, C. Fiber-optic humidity sensor based on an air-gap long period fiber grating. Opt. Rev. 2011, 18, 93–95.

64. Pissadakis, S.; Vainos, N.A.; Konstantaki, M. Thin film overlaid long period fibre grating sensors: Examples and prospects for advanced health monitoring applications. In Proceedings of the 2009 9th International Conference on Information Technology and Applications in Biomedicine, Larnaka, Cyprus, 4–7 November 2009; pp. 1–4.

65. Xia, L.; Li, L.; Li, W.; Kou, T.; Liu, D. Novel optical fiber humidity sensor based on a no-core fiber structure. Sens. Actuators A Phys. 2013, 190, 1–5.

66. Urrutia, A.; Goicoechea, J.; Rivero, P.J.; Matías, I.R.; Arregui, F.J. Electrospun nanofiber mats for evanescent optical fiber sensors. Sens. Actuators B Chem. 2013, 176, 569–576.

67. Liu, Y.; Zhang, Y.; Lei, H.; Song, J.; Chen, H.; Li, B. Growth of well-arrayed ZnO nanorods on thinned silica fiber and application for humidity sensing. Opt. Express 2012, 20, 19404–19411.

68. Alwis, L.; Sun, T.; Grattan, K. Fibre optic long period grating-based humidity sensor probe using a Michelson interferometric arrangement. Sens. Actuators B Chem. 2013, 178, 694–699.

69. Li, T.; Dong, X.; Chan, C.C.; Zhao, C.L.; Zu, P. Humidity sensor based on a multimode-fiber taper coated with polyvinyl alcohol interacting with a fiber Bragg grating. IEEE Sens. J. 2011, 12, 2205–2208.

70. Liang, H.; Jin, Y.; Wang, J.; Dong, X. Relative humidity sensor based on polarization maintaining fiber loop mirror with polymer coating. Microw. Opt. Technol. Lett. 2012, 54, 2364–2366.

71. Wong, W.C.; Chan, C.C.; Chen, L.H.; Li, T.; Lee, K.X.; Leong, K.C. Polyvinyl alcohol coated photonic crystal optical fiber sensor for humidity measurement. Sens. Actuators B Chem. 2012, 174, 563–569.

72. Mathew, J.; Semenova, Y.; Rajan, G.; Wang, P.; Farrell, G. Improving the sensitivity of a humidity sensor based on fiber bend coated with a hygroscopic coating. Opt. Laser Technol. 2011, 43, 1301–1305.

73. Zhao, Z.; Duan, Y. A low cost fiber-optic humidity sensor based on silica sol–gel film. Sens. Actuators B Chem. 2011, 160, 1340–1345.

74. Fuke, M.V.; Kanitkar, P.; Kulkarni, M.; Kale, B.; Aiyer, R. Effect of particle size variation of Ag nanoparticles in Polyaniline composite on humidity sensing. Talanta 2010, 81, 320–326.

75. Akita, S.; Sasaki, H.; Watanabe, K.; Seki, A. A humidity sensor based on a hetero-core optical fiber. Sens. Actuators B Chem. 2010, 147, 385–391.

76. Shukla, S.; Tiwari, A.; Parashar, G.; Mishra, A.; Dubey, G. Exploring fiber optic approach to sense humid environment over nano-crystalline zinc oxide film. Talanta 2009, 80, 565–571.

77. Vijayan, A.; Fuke, M.; Hawaldar, R.; Kulkarni, M.; Amalnerkar, D.; Aiyer, R. Optical fibre based humidity sensor using Co-polyaniline clad. Sens. Actuators B Chem. 2008, 129, 106–112.

78. Zhang, L.; Gu, F.; Lou, J.; Yin, X.; Tong, L. Fast detection of humidity with a subwavelength-diameter fiber taper coated with gelatin film. Opt. Express 2008, 16, 13349–13353.

79. Chen, L.H.; Chan, C.C.; Li, T.; Shaillender, M.; Neu, B.; Balamurali, P.; Menon, R.; Zu, P.; Ang, X.M.; Wong, W.C.; et al. Chitosan-coated polarization maintaining fiber-based Sagnac interferometer for relative humidity measurement. IEEE J. Sel. Top. Quantum Electron. 2012, 18, 1597–1604.